Journal of Statistical Physics, Vol. 69, Nos. 5/6, 1992

On a Discrete Model of Phase Separation Dynamics

T. Gobron[1,2]

Received November 26, 1991; final July 10, 1992

A spatially discrete model for phase separation with conserved order parameter is proposed. This one-dimensional model is obtained as the deterministic limit of an anisotropic lattice gas. A particular choice is made for the jump rates (which still fulfill detailed balance conditions) so that the resulting model is mathematically tractable. It exhibits a phase transition of first-order type whose nonlinear dynamics is investigated using both analytical and numerical methods. All the stationary solutions with zero current are found and parametrized in terms of Jacobian elliptic functions, showing a striking similarity with the nonlinear (continuous) Cahn–Hilliard equation. In the limit of infinite wavelength, particular solutions are found which descrive isolated domains of arbitrary size embedded in an homogeneous infinite medium of the opposite phase. New results are also presented on the structure of the set of solutions. Time-dependent profiles are studied in the spinodal regime and the stability of bounded stationary solutions is also investigated in this context. A description of time-dependent profiles is proposed which considers only interactions between neighboring domains and makes use of isolated domain solutions. This approach results in an analytic expression for the exponents characteristic of the instability of stationary solutions and is validated by comparison to numerical values. Qualitative results are also discussed and the relation to the Cahn–Hilliard equation is emphasized.

KEY WORDS: Phase separation dynamics; stationary solutions; discrete equations.

1. INTRODUCTION

Over the last 30 years the dynamics of phase separation has been the subject of numerous works which have successfully described some of its

[1] Laboratoire de Physique de la Matière Condensée (Unité de Recherche D1254 du CNRS), Ecole Polytechnique, 91128 Palaiseau Cedex, France.

[2] Present address: Dipartimento di Fisica, Universita "La Sapienza", Rome, Italy.

0022-4715/92/1200-0995$06.50/0

important features: initial pattern selection in the spinodal regime,[1–3] growth law of the mean domain size,[4,5] scaling properties of the structure function,[6] etc. However, the theoretical models[7] which are used in this field have been developed in a context of equilibrium statistical mechanics and are far from lying on a firm basis when dealing with macroscopically inhomogeneous nonequilibrium systems. The theoretical difficulties which arise in the use of such methods have not yet been overcome and it would be of interest to have a better understanding of their physical meaning.

In this task, new insights could be found by using simple models on which different approaches could overlap. In this paper, a spatially discrete model is proposed which we hope fulfils this requirement. It can be derived at least heuristically from an anisotropic lattice gas and in principle its dynamics could be compared to that of the initial stochastic model.[8] The jump rates of the initial lattice gas have been chosen so that the stationary solutions of the resulting lattice model can be found analytically. This property is at the origin of the particular interest in the present model, which, besides this, is presumably equivalent to other models derived within a similar scheme of approximations.[9,10] It exhibits a phase transition of first-order type whose nonlinear dynamics is investigated using both analytical and numerical methods. The present model was also found to be strongly related to the well-known Cahn–Hilliard (CH) equation.[1,2] Although no rigorous proof of a mathematical equivalence can be given, both statics and dynamics are found to be similar and this will be emphasized throughout this paper. The deeper point of divergence concerns the absence of a free energy functional in the present case and this seems to be essentially a consequence of discretization.

In Section 2, the model and its evolution equation are obtained from an anisotropic lattice gas model described by a master equation. General properties are discussed in Section 3. The phase diagram of the transition is given and preliminary comments on the relation to the CH equation are also presented. Section 4 is devoted to the analytic derivation of the stationary (zero current) solutions. This requires the resolution of an infinite set of coupled nonlinear discrete equations and is achieved through a parametrization in terms of Jacobian elliptic functions. Surprisingly, the structure of the solution is found to be the same as for the CH equation. In addition, a clear picture of the structure of the set of solutions is given whose general features are valid for both cases. Two disjoint sets of bounded solutions are found, corresponding respectively to bounded solutions inside and outside the interval $[0, 1]$. Only the first one is relevant to phase separation dynamics and exists only below the critical temperature. A duality relation is found which connects low- and high-density solutions, in analogy with the usual symmetry of the CH equation. In the limit of

infinite wavelength, two dual one-parameter families of solutions are found which describe the profile of single isolated domains of arbitrary size embedded in an infinite homogeneous medium of the other phase. When the domain size becomes infinite, both converge to the same limit in which two semi-infinite phases with asymptotic equilibrium densities are separated by a stable interface. In Section 5, numerical and analytical results on the late stages of spinodal separation are presented. Based on qualitative results of a preliminary numerical study, a description of time-dependent profiles is proposed which considers only the interaction between neighboring domains. Using the previously found isolated domain solutions, this approach leads to an analytic expression for the exponents which characterize the instability of stationary solutions, giving the dependence on both wavelength and mean concentration. Two different modes are considered, one corresponding to the fusion of high-concentration domains, the other to the fusion of low-concentration domains, and their relative importance is found to depend sharply on the mean concentration. The expression is then compared to numerical values obtained on periodic solutions, giving quantitative support to the present description. As a conclusion, a short list of possible developments of this model is given.

2. DERIVATION OF THE EVOLUTION EQUATIONS

In this section, the model is defined and its evolution equation derived from a lattice gas model which provides the underlying microscopic basis. This derivation and the approximations which are made here are already known to lead to mean-field-type models.[10,11] Here, the transition rates of the lattice gas model are chosen from an additional requirement, besides detailed balance conditions, so that the resulting evolution equation has some properties of solvability, which are the basic tool for the rest of the paper.

The general scheme of derivation is as follows: one considers a highly anisotropic lattice gas model so that the time scale of motion on a privileged axis z is much slower than the time scale for the diffusion in any perpendicular plane. Such a situation can occur, for instance, when interstitial atoms are embedded in an anisotropic matrix. In addition, we suppose that the anisotropic coupling to the matrix is such that a homogeneous equilibrium is reached independently within each plane, while the slow time dynamics along the z axis can be considered to be decoupled from that motion and reversible with respect to a pseudo-one-dimensional Ising Hamiltonian. In this case, the set of relevant degrees of freedom is reduced to the subset of mean concentrations in each perpendicular plane and the slow-scale dynamics is described by a one-dimensional stochastic model.

Then, the neglect of fluctuations, or more precisely the assumption that the probability distribution is a sharply peaked function in the neighborhood of the most probable configuration, leads to a deterministic equation for the evolution of the mean concentration in each plane. This approximation is known to lead (in the continuous case) to a generalized diffusion equation starting from a stochastic model.[12] For that reason, the resulting discrete model can be already expected to be comparable to the CH equation, as will be confirmed.

This procedure is now applied to a particular case. Consider a cubic lattice Λ whose sites are occupied by at most one particle. Any configuration of the system is fully specified by the set η of all occupation numbers, the particles being all identical:

$$\eta = \{n_i\}_{i \in \Lambda} \tag{1}$$

n_i is the occupation number on site i and takes the value 1 or 0 according to the presence or not of a particle on that site. The time evolution is specified from a stochastic point of view by a master equation which determines the variations of the probability $P(\eta, t)$ of finding the system in a configuration η at time t:

$$\frac{\partial}{\partial t} P(\eta, t) = \sum_{\eta'} \{W(\eta' \to \eta)\, P(\eta', t) - W(\eta \to \eta')\, P(\eta, t)\} \tag{2}$$

All the dynamical information is contained in the transition rates $W(\eta \to \eta')$ which give the probability per unit time for the system to evolve from configuration η to configuration η'. In order to describe the motion of particles by elementary jumps, those rates are all set to zero except when the initial and final configurations differ only by the interchange of a pair of occupation numbers on two neighboring sites. The transition rates are chosen as follows: when the attempted jump is parallel to the z axis, the jump rate $W^{\parallel}$ is assumed to fulfil detailed balance conditions with respect to a pseudo-one-dimensional Ising Hamiltonian $H(\eta) = -J \sum_i n_i n_{i+\mathbf{u}}$, where the sum is over all lattice sites, $\mathbf{u}$ is the unit vector on the z axis, and J is a positive coupling constant. This does not completely specify the parallel jump rates and we further assume the following particular form:

$$W^{\parallel}(\eta \to \eta') = \nu_0 \sum_{i \in \Lambda} \sum_{\delta = \pm \mathbf{u}} \delta(\eta^{i, i+\delta}, \eta')\, n_i (1 - n_{i+\delta}) \exp(-\beta J n_{i-\delta}) \tag{3}$$

where $\eta^{i,j}$ is defined as the configuration deduced from η by exchanging the occupation numbers at sites i and j, β is the inverse temperature, and ν_0 is a jump frequency. The factor $n_i(1 - n_{i+\delta})$ ensures particle conservation and exclusion of double occupation.

A complete physical description of the in-plane motion cannot be stated within the lattice gas model, as it involves nontrivial contributions from the imbedding matrix. Here, it will be simply assumed that the jump rates $W^{\perp}$ which govern jumps in the direction perpendicular to the z axis are large enough and sufficiently decoupled from the Hamiltonian description of the z motion to destroy all the in-plane correlations in the slow time scale. The simplest (and very rough) way of taking this into account would be to assume a large constant in-plane jump attempt frequency (together with exclusion of double occupation). Then in some limit of infinite separation between the two time scales, any two configurations with the same number of particles in each plane will have the same probability on the slow time scale and the details of the configurations inside the planes will become irrelevant. Therefore, only the number of particles or equivalently the mean concentration ρ_k on each plane k has to be retained and one can define an "averaged" configuration ξ as the one-dimensional set of these mean concentrations,

$$\xi \equiv \{\rho_k\}_{k \in \mathbb{Z}} \tag{4}$$

Within this kind of approximation, the model reduces to a pseudo-one-dimensional stochastic lattice model for the continuous variables ρ_k. The time evolution of the probabilities of the averaged configurations ξ is described by a new master equation which reads

$$\frac{\partial}{\partial t} P(\xi, t) = \sum_{\xi'} \{\overline{W^{\parallel}}(\xi' \to \xi)\, P(\xi', t) - \overline{W^{\parallel}}(\xi \to \xi')\, P(\xi, t)\} \tag{5}$$

where the averaged transition rates $\overline{W^{\parallel}}(\xi \to \xi')$ connect two configurations differing only by the exchange of one particle between two adjacent planes, irrespective of its actual position within those planes. Let ξ' be the configuration differing from ξ by taking out one particle in the plane k and putting one more in the neighboring plane $k+\delta$. The averaged transition rate between them, $\overline{W^{\parallel}}(\xi \to \xi')$, is obtained from Eq. (3) by summing over all the configurations which contribute (with the same weight) to this transition and reads

$$\overline{W^{\parallel}}(\xi \to \xi') = \nu_0[1 + \rho_{k-\delta}(e^{-\beta J} - 1)]\, \rho_k(1 - \rho_{k+\delta}) \tag{6}$$

Now, if the distribution $P(\xi, t)$ is a sharply peaked function around a given averaged configuration $\{\rho_k\}$, the fluctuations can be neglected in first approximation and a deterministic equation for the time evolution of the ρ_k is obtained as the first moment of the previous master equation:

$$\frac{\partial}{\partial t} \rho_k = \sum_{\delta = \pm 1} \{(1 + K\rho_{k+2\delta})\, \rho_{k+\delta}(1 - \rho_k) - (1 + K\rho_{k-\delta})\, \rho_k(1 - \rho_{k+\delta})\} \tag{7}$$

where K is a temperature-dependent parameter:

$$K = e^{-\beta J} - 1 \tag{8}$$

and ranges from -1 at zero temperature to 0 at infinite temperature. The lattice spacing has been taken equal to 1 and the time unit has been rescaled so that in the infinite-temperature limit ($K=0$), the diffusion coefficient equals one in units of (lattice spacing)^2 per unit time.

The rest of the article is devoted to the study of the above deterministic equation. In particular, spinodal decomposition in the nonlinear regime of dynamics will be explored. For that purpose, noise effects are known to be irrelevant[13] and the present restriction to the deterministic part is then well founded. Nevertheless, a comparison with the lattice gas dynamics might well be of great interest, in particular in the study of metastability. The present model (and the analytical results to be obtained on it) could also be used backward to determine precisely the effects of the approximations made in its derivation.

3. GENERAL PROPERTIES

The present section will be mostly devoted to the definition of spinodal line and coexistence curve, as well as the basic mathematical properties of Eq. (7), which will be the starting point of next section. First, one can remark that Eq. (7) can be cast in the form of a local conservation equation for the concentration on each site k:

$$\frac{\partial}{\partial t}\rho_k = -(J_{k,k+1} - J_{k-1,k}) \tag{9}$$

where the right-hand side has the form of a discrete gradient and the function $J_{k,k+1}$ is the current between sites k and $k+1$:

$$J_{k,k+1} = [1 + K\rho_{k-1}]\,\rho_k[1-\rho_{k+1}] - [1 + K\rho_{k+2}]\,\rho_{k+1}[1-\rho_k] \tag{10}$$

From Eq. (9), it is easy to show that the total concentration of a closed system will be exactly conserved in time as for the CH equation. A closer comparison can be made by looking at the long-wavelength behavior of Eq. (7). In this limit, the presence of the lattice is not important and the concentrations ρ_k can be considered as depending on a continuous spatial coordinate z. Up to the second order in the lattice spacing, Eq. (7) can be then approximated by the following nonlinear diffusion equation:

$$\frac{\partial \rho}{\partial t} = \frac{\partial}{\partial z}\left[D(\rho)\frac{\partial \rho}{\partial z}\right] \tag{11}$$

where $D(\rho)$ is a concentration-dependent diffusion coefficient:

$$D(\rho) = 1 + 4K\rho - 3K\rho^2 \tag{12}$$

In this limit, the evolution equation exhibits further similarities with the CH equation. Up to this second order, both equations are equivalent and two different dynamics show up according to the sign of $D(\rho)$: for positive values, the behavior of small enough perturbations can be shown to be purely diffusive and correctly described by Eq. (11); for negative values, Eq. (11) becomes unstable under arbitrary small perturbations of homogeneous profiles and corrective terms have to be added to avoid inconsistency. In the CH equation, a fourth-order term (a phenomenological surface tension) is present which stabilize the equation. Here, a further development to higher-order terms in lattice spacing could be a way of adding corrective terms in the right-hand side of Eq. (11). However, it is not clear whether this is sufficient to describe the discrete model and in particular to prove that its behavior is regular in the spinodal region. On that last point, one can only rely on numerical simulations.

Separating the two regimes, a spinodal line can be defined using Eq. (12) as the locus of the zeros of $D(\rho)$ in the (ρ, K) plane (Fig. 1). This also defines a critical point at temperature $K_c = -3/4$ and concentration $\rho_c = 2/3$.

Besides these results obtained in the infinite-wavelength limit, a linear stability analysis can be performed around homogeneous profiles within

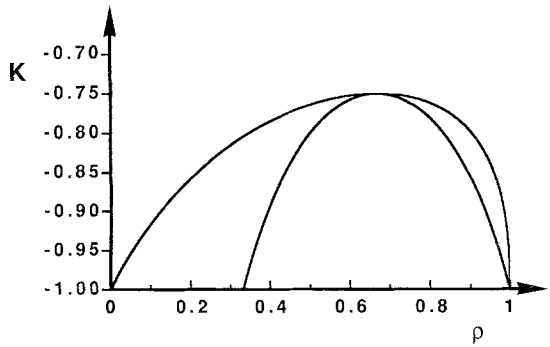

Fig. 1. Phase diagram. K is a temperature-dependent external parameter ranging from -1 at zero temperature to 0 at infinite temperature. The spinodal line locates the values for which the diffusion coefficient is zero. The coexistence curve is obtained from necessary conditions for the existence of a stationary solution connecting two homogeneous phases. This defines three regions associated to different dynamics of quasihomogeneous profiles: diffusive (above the coexistence curve), metastable, and unstable (inside the spinodal curve). The critical point is located at $\rho_c = 2/3$ and $K_c = -3/4$.

the discrete model itself. For that purpose, one considers a homogeneous infinite system at concentration ρ on which has been added a periodic perturbation $\delta\rho_k(t)$:

$$\delta\rho_k(t) = \varepsilon(t)\cos(2\pi\nu k) \tag{13}$$

where ν is the wavenumber of the periodic perturbation, k the coordinate on the lattice, and $\varepsilon(t)$ a small time-dependent amplitude. A first-order development of Eq. (7) shows that the amplitude of the perturbation grows (or decays) exponentially with time, $\varepsilon(t) \propto \exp(\omega t)$, and that the growth rate ω is related to the wavenumber ν through the following dispersion relation:

$$\omega = -2[1-\cos(2\pi\nu)]\{(1+4K\rho-3K\rho^2)-2K\rho(1-\rho)[1-\cos(2\pi\nu)]\} \tag{14}$$

In the long-wavelength limit ($\nu \to 0$), one recovers the fact that the perturbation grows only in the region where $D(\rho)$ is negative:

$$\omega = -4\pi^2\nu^2 D(\rho) \tag{15}$$

Both discrete and continuous equations (7) and (11) define the same spinodal line because the onset of instability always occurs at infinite wavelength. However, inside the spinodal region, the instability develops at finite wavelength and the values of the growth rates (Fig. 2) are different.

The major difference between Eq. (7) and the Cahn–Hilliard equation seems to be of structural nature: The point is that no (local) free energy

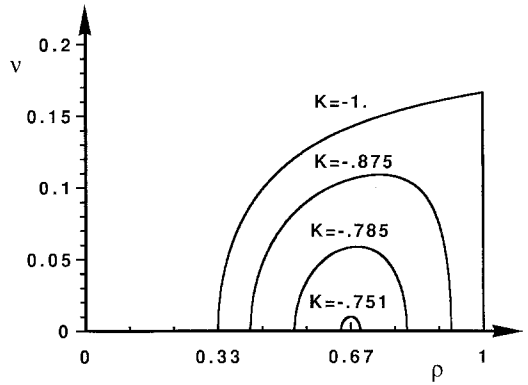

Fig. 2. Wavenumber ν (inverse of the wavelength) associated to the most unstable mode of homogeneous profiles. ν is represented as a function of concentration for different values of K and is expressed in units of inverse lattice spacing. These modes characterize the first stages of spinodal decomposition (see Fig. 6a).

functional can be constructed from which Eq. (7) could be derived. Even introducing a free energy functional in the infinite-wavelength limit is not so easy and the value of the coexistence curve which can be precisely found in numerical simulations could not be derived in that way. As a counterpart, the model exhibits a remarkable property associated to its discrete character, and in relation to which the particular choice of jump rates [Eq. (3)] was made: if one tries to write now the previously defined current $J_{k,k+1}$ as the product of a concentration-dependent mobility $M_{k,k+1}$ and the (discrete) gradient of a chemical potential μ_k,

$$J_{k,k+1} = -M_{k,k+1}(\mu_{k+1} - \mu_k) \tag{16}$$

one finds that this factorization is not only possible, but that it can be done in different ways. For instance, it is easy to verify that the two choices $(\mu_k^a, M_{k,k+1}^a)$, $(\mu_k^b, M_{k,k+1}^b)$ hold, where

$$\mu_k^a = \rho_k[1 + K(\rho_{k-1} + \rho_{k+1}) - K\rho_{k-1}\rho_{k+1}] \tag{17a}$$

$$M_{k,k+1}^a = 1 \tag{17b}$$

and

$$\mu_k^b = \frac{(1 + K\rho_k\rho_{k+1})(1 + K\rho_k\rho_{k-1})}{1 - \rho_k} \tag{18a}$$

$$M_{k,k+1}^b = \frac{(1 - \rho_{k+1})(1 - \rho_k)}{1 + K\rho_k\rho_{k+1}} \tag{18b}$$

It can be also demonstrated that any algebraic function of μ_k^a and μ_k^b solves Eq. (16) and that there is no other independent solution than these two. In the absence of any free energy functional from which a distinction could be made, a special choice of $\{\mu_k\}$ cannot be elicited as the true chemical potential and in the following all these functions will by abuse of language be called "chemical potentials" (between quotes) by reference to Eq. (16).

This multiplicity of decompositions is a very specific property of Eq. (7) and gives the model some unique properties of solvability which contribute in large part to its interest. For instance, the coexistence curve can be defined from the necessary condition that each "chemical potential" must have the same value in two homogeneous phases in equilibrium. Here, two independent relations can be written which relate the densities ρ_+ and ρ_- of the coexisting phases:

$$\mu^a(\rho_+) = \mu^a(\rho_-) \tag{19a}$$

$$\mu^b(\rho_+) = \mu^b(\rho_-) \tag{19b}$$

These two independent relations allow for the determination of ρ_+ and ρ_- as a function of temperature:

$$\rho_\pm = \frac{-1}{2K}\left[1 \pm (-4K-3)^{1/2}\right] \tag{20}$$

The resulting coexistence curve has been drawn, together with the spinodal line, on Fig. 1 and defines the same value for the critical point. The values of the "chemical potentials" on the coexistence curve can be also determined:

$$A_c \equiv \mu^a(\rho_\pm) = -\frac{(K+1)(2K+1)}{K^2} \tag{21}$$

$$B_c \equiv \mu^b(\rho_\pm) = -\frac{1}{K} \tag{22}$$

However, it should be noted that the coexistence curve has been defined only through necessary conditions and that its existence remains to be proven. In the next section, Eqs. (17)–(18) will be used to derive the full set of stationary solutions with zero current. In particular, a solution will be found which connects the two coexisting homogeneous phases by a single interface. In the last section, it will be shown that this is actually the only stable equilibrium profile in the spinodal region.

4. STATIONARY SOLUTIONS

In this section, the time-independent solutions of Eq. (7) with zero current will be given explicitly and parametrized in term of Jacobian elliptic functions. In what follows, the discussion is undertaken in order to avoid a too technical presentation and requires only basic definitions and properties of elliptic functions which can be easily found in the literature[14,15] in the same standard notations.

Starting from the requirement that the current $J_{k,k+1}$ is null everywhere along a given solution classically leads through Eq. (16) to the well-known fact that the chemical potential μ_k is constant for all the values of k. Due to the multiplicity in the definition of the "chemical potential" described in the previous section, one is led here not to one but to two sets of independent relations. Let A (respectively B) be the constant value taken by μ_k^a (respectively μ_k^b) along the stationary solution. Using Eqs. (17) and (18), one finds that the concentrations on any triplet of successive sites

$k-1, k, k+1$ are related through the two following equations, valid for all values of k:

$$\rho_k(1+K\rho_{k-1}+K\rho_{k+1}-K\rho_{k-1}\rho_{k+1})=A \tag{23}$$

$$\frac{(1+K\rho_{k-1}\rho_k)(1+K\rho_k\rho_{k+1})}{1-\rho_k}=B \tag{24}$$

where A and B are hence two constants (independent of k) characteristic of a given stationary solution.

A first (discrete) integration of these equations is performed when one variable, say ρ_{k-1}, is eliminated between Eqs. (23) and (24). This results into the following equation, which holds on each pair of nearest neighboring sites k, $k+1$:

$$K^2\rho_k^2\rho_{k+1}^2+K\rho_k\rho_{k+1}(\rho_k+\rho_{k+1})+(B-KA)\,\rho_k\rho_{k+1}+(1-B)\times(\rho_k+\rho_{k+1})+(B-A-1)=0 \tag{25}$$

The left-hand side of Eq. (25) has the form of a symmetrical polynomial of second order in both variables and a similar form would have been found if another choice of the variable to be eliminated was done. However, Eq. (25) (for all k's) is not exactly equivalent to the previous set, Eqs. (23) and (24), and some specifications on its valid solutions have to be added, which can be already stated in the following way: any solution of Eq. (25) (for all k's) can be constructed by iteration with increasing values of k. In this process, the value of ρ_{k+1} is not uniquely determined by the value of ρ_k and can be chosen at each step among two solutions. In fact, Eqs. (23) and (24) must be used to define the choice to be made, and this imposes ρ_{k+1} as the only solution of Eq. (25), for k and ρ_k fixed, which is distinct from ρ_{k-1}. This amounts only to avoiding spurious retrogression points in the iteration and will be taken into account in the following.

Interest in Eq. (25) is that it can be linearized by introducing a parametrization in terms of Jacobian elliptic functions, and hence solved simultaneously for all k's. This is achieved in two steps. The first one is an algebraic change of parameters which permits one to reduce the multiplicities in the parametrization and to introduce the elliptic parameters. One looks for a change of variables in the form

$$\rho_k=\xi\frac{u_k-c_0}{u_k-c_1} \tag{26}$$

where the constants c_0, c_1, and ξ have to be chosen so that Eq. (25) becomes equivalent to a canonical recurrence equation of the form

$$(1-a^2)\,u_k^2u_{k+1}^2+2abu_ku_{k+1}-u_k^2-u_{k+1}^2+(1-b^2)=0 \tag{27}$$

which form is motivated by the elliptic parametrization to be introduced later. The equivalence between Eq. (25) and Eq. (27) is expressed by equating the two left-hand sides up to a nonvanishing proportionality factor. This gives a set of five equations from which one can extract both the parameters a and b and the constants c_0, c_1, and ξ, proving ipso facto the existence of such a transformation, though not free of multiplicities. After some transformations, the constants c_0, c_1, and ξ can be eliminated from two of the five equations and one finds that the pair of parameters (a, b) is any solution of the following equations:

$$\frac{B}{AK} = \frac{2(a+b)^2}{ab(a^2b^2 - a^2 - b^2)} \tag{28}$$

$$\frac{(B-AK)^2}{4K[AK+(K+1)(1-B)]} = \frac{(ab+2)^2}{(a+b)^2 - a^2b^2} \tag{29}$$

These two equations define a correspondence between the two pairs (A, B) and (a, b), showing that, up to some multiplicities, a given stationary solution can be equivalently characterized by either of the two sets of parameters. As will appear clearly later, the (a, b) parametrization is more appropriate and is therefore used in the following. Hence, in order to start with a well-defined correspondence, multiplicities have to be checked in Eqs. (28) and (29), showing two different aspects: first, one finds that there are generally 12 different solutions (a, b) for a given choice of A and B (K fixed). Fortunately, a study of the transformations leaving invariant the right-hand sides of Eqs. (28) and (29) shows that these equations have one and only one solution (a, b) in the domain of the real plane defined by $\{b < 1, a > |b|\}$ (Fig. 3) when A and B are real. In the following, a restriction of the values of (a, b) to that domain is assumed, which eliminates all the possible multiplicities in the elliptic parametrization of a same solution. Conversely, given the values of (a, b) and K being fixed, Eqs. (28) and (29) define generally two distinct values of (A, B). Here, the multiplicity makes sense, as distinct values of (A, B) define different solutions. It will be proved that this defines pairs of stationary solutions which share a number of properties and must be considered as dual one to another.

The second step in the explicit derivation of a stationary solution consists in introducing the elliptic parametrization through Eq. (27). First, the parameters a and b are written as two different elliptic functions of same parameter m and argument ϕ as

$$a = \mathrm{dn}(\phi, m) \tag{30}$$

$$b = \mathrm{cn}(\phi, m) \tag{31}$$

There is some arbitrariness in this choice, but there is no loss of generality, provided that the general definition of Jacobian elliptic functions is considered in which the parameter m can take any real value and the argument ϕ any complex value. This allows us to cast the parametrization of stationary solutions into a single case and avoid an otherwise cumbersome (and not simpler) discussion of different cases. Furthermore, the choice of Eqs. (30) and (31) fits into a more restrictive definition ($m \in [0, 1]$, $\phi \in \mathbb{R}$) for bounded real solutions. In any case, Eqs. (30) and (31) can be inverted: first, the parameter m can be defined as the ratio

$$m = \frac{1-a^2}{1-b^2} \tag{32}$$

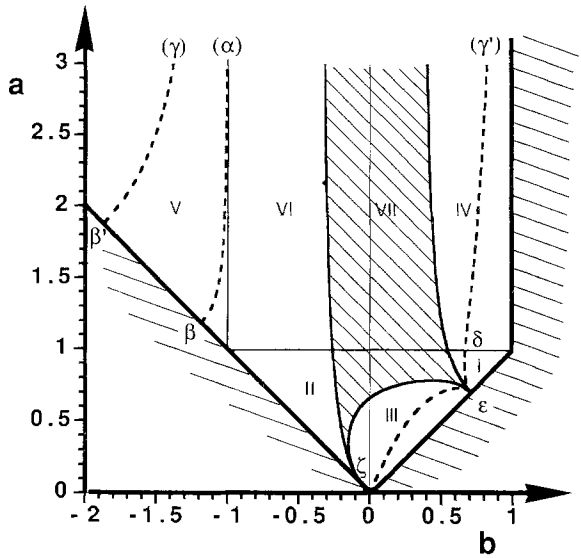

Fig. 3. Domain of parametrization $\{a, b \in \mathscr{R};\ a > |b|, b < 1\}$ of the set of real stationary solutions and its temperature-dependent partition below the critical point, for $K = -0.875$. This domain is separated into seven regions whose boundaries correspond to particular (degenerate) solutions. Each point (a, b) in this domain defines at most four stationary solutions of the same wavelength. These solutions can be associated in pairs of dual solutions, each associated to a different value of the initial parameters (A, B). The shaded region VII contains no real solutions and regions III, IV, V, and VI only real unbounded solutions of different types. In regions I and II, each point (a, b) defines a pair of dual bounded solutions and a pair of dual unbounded solutions with a gap. Region II contains all bounded solutions evaluated outside $[0, 1]$. Region I contains all bounded solutions in $[0, 1]$ and vanishes at the critical temperature. The dashed curve locates the points on which the "chemical potential" $A = A_c$. The value of B varies continuously from $-\infty$ at (α) to $+\infty$ at ζ. Two discontinuities appear in β, β' $(B = 0)$ and γ, γ' $[B = -(K+1)/K]$, related to the planar representation. Point ε $(B = -1/K)$ locates the coexistence curve and δ $[B = -(K+1)(4K+1)^2/K]$ defines a homogeneous solution. A third discontinuity, of physical nature, appears around point ε when A is slightly varied.

Then, m being fixed, ϕ can be found by inverting either Eq. (30) or Eq. (31). The above elliptic functions being both periodic and even, the value of ϕ is defined only up to a sign and modulo the real and imaginary periods of the elliptic functions, hereafter denoted as $4\mathcal{K}(m)$ and $4i\mathcal{K}'(m)$. The choice of a particular determination of ϕ, however, has no influence on the parametrization.

Now, still without loss of generality, the variables u_k which appear in Eq. (27) can be also written for each value of k as a third elliptic function with the same parameter m; the argument α_k is defined modulo $4\mathcal{K}(m)$ and $2i\mathcal{K}'(m)$ from

$$u_k = \mathrm{sn}(\alpha_k, m) \tag{33}$$

Using these notations and considering Eq. (27) as a second-order polynomial equation in u_{k+1}, one can remark that its normalized coefficients are exactly the sum and product of $\mathrm{sn}(\alpha_k - \phi)$ and $\mathrm{sn}(\alpha_k + \phi)$. This gives a straightforward (though not unique) way of factorizing the left-hand side of Eq. (27) as

$$[-1 + m\,\mathrm{sn}(\alpha_k)^2\,\mathrm{sn}(\phi)^2][\mathrm{sn}(\alpha_{k+1}) - \mathrm{sn}(\alpha_k + \phi)][\mathrm{sn}(\alpha_{k+1}) - \mathrm{sn}(\alpha_k - \phi)] = 0 \tag{34}$$

where a dependence of the elliptic functions on the parameter m is implicit. This factorization is well defined whenever the first factor in Eq. (34) is nonzero and Eq. (27) can be solved directly otherwise. In all cases, the value of α_{k+1} can be related to that of α_k as

$$\alpha_{k+1} = \alpha_k \pm \phi \tag{35}$$

This equality is in fact defined modulo the periods of $\mathrm{sn}(\cdot)$, but Eq. (33) does not require much more. Now recalling that u_{k+1} and u_{k-1} should be the two generically distinct solutions of Eq. (27) [see below, Eq. (25)], this imposes the choice of a constant sign of the increment in Eq. (35) for all k's. Therefore, a valid general solution of Eq. (27) reads

$$u_k = \mathrm{sn}(k\phi + \Psi, m), \qquad k \in \mathbb{Z} \tag{36}$$

where Ψ is an arbitrary phase which can possibly absorb a change in the sign of ϕ and whose value will be discussed later.

In order to complete the derivation, the constants c_0, c_1, and ξ which define the transformation (27) have now to be given. They are solutions of three equations which along with Eqs. (28) and (29) define the equivalence between Eqs. (25) and (27). Using the same elliptic parametrization and

after some algebra, it can be shown that they can be all expressed with the help of a single new angle $\Theta \in \mathbb{C}$ as

$$c_0 = \mathrm{sn}(\Theta - 3\phi/2, m) \tag{37}$$

$$c_1 = \mathrm{sn}(\Theta - \phi/2, m) \tag{38}$$

$$\xi = \frac{\mathrm{sn}(\Theta + 3\phi/2, m) - \mathrm{sn}(\Theta - \phi/2, m)}{\mathrm{sn}(\Theta + 3\phi/2, m) - \mathrm{sn}(\Theta - 3\phi/2, m)} \tag{39}$$

where Θ is a solution of the following equation:

$$\left(\frac{\mathrm{sn}(\Theta, m)}{\mathrm{cn}(\Theta, m)\,\mathrm{dn}(\Theta, m)}\right)^2 = \frac{(1-b^2)[(K+1)(a+b)^2 - a^2b^2]}{K(a+b)^2\,(a-b)^2} \tag{40}$$

To summarize, one can now use Eq. (27) together with Eqs. (37)–(39) and write the general form of a stationary solution $\{\rho_k\}_{k \in \mathbb{Z}}$ of the evolution equation (7) as

$$\rho_k = \frac{\mathrm{sn}(\Theta + 3\phi/2, m) - \mathrm{sn}(\Theta - \phi/2, m)}{\mathrm{sn}(\Theta + 3\phi/2, m) - \mathrm{sn}(\Theta - 3\phi/2, m)} \times \frac{\mathrm{sn}(\Psi + k\phi, m) - \mathrm{sn}(\Theta - 3\phi/2, m)}{\mathrm{sn}(\Psi + k\phi, m) - \mathrm{sn}(\Theta - \phi/2, m)} \tag{41}$$

for all k's, provided that m, ϕ (or equivalently a, b), and Θ are related through the temperature-dependent equation (40).

It is worth noting that Eq. (41) shows the same spatial dependence of stationary solutions as the Cahn–Hilliard equation,[16,17] although one deals here with discrete equations. In addition, a precise picture of the structure of the set of stationary solutions, valid for both cases, can be given and is further described below.

First, the stationary solutions are almost all periodic and this follows directly from the expression given by Eq. (41) and general properties of elliptic functions. The only aperiodic solutions correspond to the value $m = +1$ and can be attained continuously from periodic solutions in the limit of an infinite period. The presence of the lattice requires this notion of periodicity to be more precisely defined as either a "true periodicity" or a "quasiperiodicity" according to the commensurability with the lattice spacing.

The general set of stationary solutions, as given by Eqs. (40) and (41), has now to be reduced to real-valued solutions, which are of primary interest. This restriction implies simply a reduction of the arbitrariness of Ψ, which until now has been unspecified. A detailed derivation will not

be given here, because this would involve a separate study for each non-equivalent domain of parametrization. However, all cases are alike and it can be shown that Ψ must be chosen so that at least one of the ratios $(\Psi \pm \Theta)/\phi$ or $[\Psi \pm \Theta \pm i\mathcal{K}'(m)]/\phi$ is real for a suitable representation of the angles Ψ, Θ , and ϕ. This implies that the further allowed changes in the value of Ψ have to be of the form $\Psi \to \Psi + \alpha\phi$, $\alpha \in \mathbb{R}$, and hence induce only off-lattice translations in Eq. (41). This degree of freedom generates a continuous family of distinct solutions in cases of true periodicity, or amounts to an indefinite on-lattice translation when the initial solution is quasiperiodic. In the following, these possible transformations will not be explicitly taken into account and all the solutions related through such transformations will be considered as a single one.

Now we can discuss the values of the parameters a and b. As can be checked directly from Eqs. (28) and (29), there exists a region in the (a, b) domain which corresponds to imaginary values of A and B and hence contains no real solutions. This leads to a temperature-dependent partition which is conveniently augmented to a set of seven distinct regions as depicted in Fig. 3 for a value of K below the critical temperature. In this representation, any real stationary solutions can be constructed first by choosing a point in the (a, b) domain outside region VII, and then one solution Θ of Eq. (40), which defines all the parameters of Eq. (41) up to an off-lattice translation.

Equation (40) admits four different solutions Θ which can be deduced one from another through two involutions. The first one, $\Theta \to \Theta + i\mathcal{K}'(m)$, where $i\mathcal{K}'(m)$ is the imaginary quarterperiod, preserves the value of the initial parameters A and B. The second one, $\Theta \to -\Theta$ (with a fixed determination of the sign of ϕ), corresponds to a change in the values of A and B and is the duality relation previously introduced.

Two cases must be distinguished, depending on whether the transformation $\Theta \to \Theta + i\mathcal{K}'(m)$ is equivalent in Eq. (41) to a translation $\Psi \to \Psi + \alpha\phi$, $\alpha \in \mathbb{R}$. When the above equivalence is true, the number of distinct solutions due to the multiplicity in the choice of Θ is reduced by a factor two and each point (a, b) defines a single pair of dual solutions. In such cases, the right-hand side of Eq. (41) has always a pole (possibly off-lattice) when k is varied over $\mathbb{Z}$. Then, all the corresponding (quasi-periodic) solutions are unbounded and it can be shown that they attain all real values. This applies to regions III, IV, V, and VI, which have still to be distinguished because each corresponds to a different type of parameterization and defines different structures of solutions.

In the other case (regions I and II), the four distinct values of Θ generate two pairs of dual solutions. In the first pair (the suitable representations of) the ratios $[\Psi \pm \Theta \pm i\mathcal{K}'(m)]/\phi$ are real and the right-hand side

of Eq. (41) has neither zeros nor poles, even off-lattice. The corresponding stationary solutions are then bounded on an interval. The second pair corresponds to real values of the ratios $(\Psi \pm \Theta)/\phi$ and defines unbounded solutions characterized by a gap in the values they can attain. It can be further proved that region I, which exists only below the critical temperature, contains all bounded solutions evaluated inside the interval [0, 1] and relevant to the problem of phase separation. All other bounded solutions are evaluated outside the interval [0, 1] and belong to region II.

In order to give a clear picture of the solutions, two kinds of representation are given. In Figs. 4 and 5, phase portraits of stationary solutions[18] are presented which show the typical topology around region I (one elliptic and two hyperbolic points). The correspondence between bounded and unbounded solutions of region I and between dual solutions is also shown. These phase portraits have been drawn by plotting in the same plane a

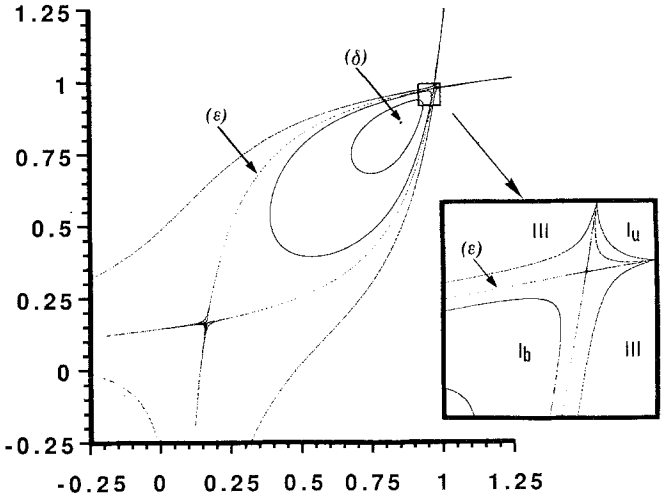

Fig. 4. Phase portrait of stationary solutions [iterates of Eq. (23) in the plane ρ_k, ρ_{k+1}] for the critical value of the "chemical potential" $A = A_c$ and different initial points ($K = -0.875$). Each orbit is associated to a particular point on the dashed curve of Fig. 3. The elliptic point is associated to point δ on the upper edge of region I. The two hyperbolic points give the concentration on the coexistence curve. The bounded and unbounded solutions associated to point ε are, respectively, the finite and infinite branches of the orbits connecting the two hyperbolic points. The finite branches are the one-kink equilibrium solution of the model (with two orientations) and the hyperbolic points define the coexistence values. Closed orbits are quasiperiodic bounded solutions and correspond to inner points of region I. Inset: the vicinity of the upper hyperbolic point has been magnified. The critical orbit separates bounded solutions (I_b) from unbounded solutions (I_u) with the same parameters [same values of A and B and same point in region I, corresponding to the transformation $\Theta \to \Theta + i\mathscr{K}'(m)$] and from unbounded solutions of region III.

large number of successive values of (ρ_k, ρ_{k+1}), which have been obtained numerically by iterating Eq. (23) for a given value of A and different initial points. The correspondence with the representation in the (a, b) domain is shown in the case $A = A_c$, which is depicted both as a phase portrait in Fig. 4 and as a single curve in Fig. 3, proving that the particular points of the latter are the particular orbits of the former. Figure 5 corresponds to a slightly different value of A.

The set of bounded solutions of region I is of particular importance and must be described in more detail. These solutions can be alternatively defined by their wavelength $\mathscr{L}$ and mean concentration ρ as

$$\mathscr{L} = \frac{4\mathscr{K}(m)}{|\phi|} = \frac{4F[\pi/2, m]}{F[\mathrm{Arccos}(b), m]} \tag{42}$$

$$\rho = \xi \left[1 + \frac{c_1 - c_2}{c_2} \frac{\Pi[1/c_2^2, m]}{F[\pi/2, m]} \right] \tag{43}$$

where $F[\cdot, m]$ and $\Pi[\cdot, m]$ are, respectively, elliptic integrals[14] of first and third kind. In order to render more explicit the dependence on the parameters a and b, the particular solutions defined on the boundaries of

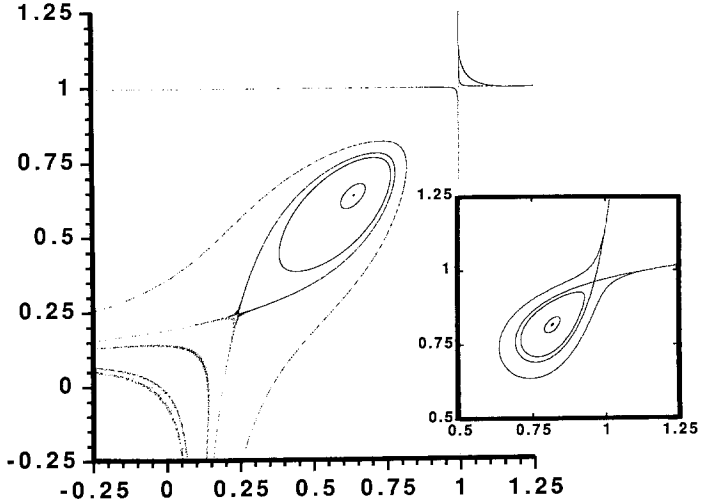

Fig. 5. Phase portrait of stationary solutions for a slightly higher value of the "chemical potential" $A = A_c + 0.03$ and the same value of temperature $K = -0.875$. The two hyperbolic points are no longer connected (which corresponds to a discontinuity around point ε) and the bounded critical orbit describes a single high-concentration domain in a homogeneous low-concentration phase. Inset: the dual orbits obtained by the transformation $\Theta \to -\Theta$ (corresponding to a change in the values of A and B). Solutions are left almost unchanged except for the exchange between high and low concentrations.

region I have been more studied. In addition, the concentration range of stationary solutions has been plotted in Fig. 6a as a function of a and b, showing the general behavior.

The uppermost edge of region I is a segment of the line $a = 1$, so that the parameter m equals 0 and elliptic functions reduce to circular ones. On this segment, all bounded solutions are constant and such a vanishing in their amplitude can be explained by the discontinuity in the order of multiplicity of Eq. (40) between region I and region IV. These constant solutions are the elliptic points in phase portraits and the zero-frequency modes of the linear stability analysis [Eq. (14)] for the associated wavenumber $v = 1/\mathscr{L} = \text{Arccos}(b)/2\pi$. All the concentration range inside the spinodal domain is covered and the two values of the spinodal line are simultaneously attained by the dual solutions defined for $a = b = 1$ ($v = 0$).

The leftmost lower edge is the border with region VII and defines self-dual stationary solutions. Accordingly, there is only one bounded solution [$\Theta = i\mathscr{K}'(m)$] defined on each point, starting from a constant solution and the smallest-wavelength limit at $a = 1$ and ending on the line $a = b$ with the infinite-wavelength solution which defines the coexistence curve. The concentration profiles of some solutions are drawn in Fig. 6b, showing the variations of both concentration range and wavelength.

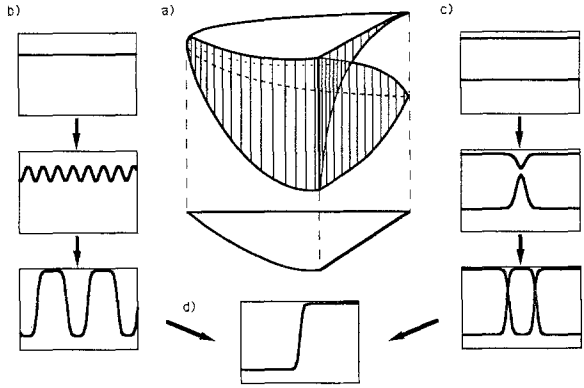

Fig. 6. Bounded stationary solutions of region I ($K = -0.875$). (a) The concentration range of the bounded solutions has been plotted on a vertical axis as a function of a and b. Due to the presence of two dual solutions on each point, this defines two intervals above each point (a, b), progressively merging into one another when the self-dual line is approached. (b, c) Concentration profiles of particular solutions defined on the boundaries of region I. The concentration scale has been reduced by a factor 1/2 from the scale of (a) and all drawings have a width of 50 sites. (b) Self-dual solutions [left boundary of (a); (c) infinite-wavelength solutions [right boundary of (a)]. Both sequences start from homogeneous solutions [smallest-wavelength limit in (b) and values at the spinodal in (c)] and end on the same equilibrium profile (d), which connects the two phases defined by the coexistence curve.

The third edge is the segment of the line $a=b$ corresponding to values between $a=2(K+1)^{1/2}$ and $a=1$. There the stationary solutions can be parametrized in terms of hyperbolic functions ($m=1$) and have an infinite period. In phase portraits, they correspond to the limiting bounded orbits attached to a hyperbolic point. Each point (a, b) defines two such dual solutions which describe a single stationary domain of high or low concentration embedded in a homogeneous infinite medium of the opposite phase. The concentration range varies across the metastability region from the values on the spinodal at $a=b=1$ to the values on the coexistence curve for $a=b=2(K+1)^{1/2}$. Some concentration profiles are drawn in Fig. 6c, showing the variation in width and amplitude of domains from spinodal line to coexistence curve.

Due to their interest and by anticipation of their use in the next section, the explicit form of these infinite-wavelength solutions will be given. It can be obtained from Eqs. (40) and (41) in the limit $m \to 1$, but a change of parameters $\Theta' = \Theta - i\mathscr{K}'(m) - \mathscr{K}(m)$ and $\Psi' = \Psi - \mathscr{K}(m)$ has to be introduced before taking that limit in order to avoid indeterminacy. $\mathscr{K}(m)$ is the real quarterperiod of elliptic functions and goes to infinity when m tends to 1. Then the solutions for $m=1$ are found in a form similar to Eq. (41) as

$$\rho_k = \frac{\cosh(2\Theta'+3\phi)-\cosh(2\Theta'-\phi)}{\cosh(2\Theta'+3\phi)-\cosh(2\Theta'-3\phi)} \times \frac{\cosh(2k\phi+2\Psi')+\cosh(2\Theta'-3\phi)}{\cosh(2k\phi+2\Psi')+\cosh(2\Theta'-\phi)} \tag{44}$$

where ϕ is related to a (or equivalently to b) through the relation

$$\phi = \operatorname{Arccosh}(1/a) \tag{45}$$

and taken as positive in the following. Θ' can take two values differing by a sign:

$$\Theta' = \pm\frac{1}{2}\operatorname{Arcsinh}\left[\left(\frac{K(\cosh^2(2\phi)-1)}{2(K+1)\cosh(2\phi)+2K+1}\right)^{1/2}\right] \tag{46}$$

The negative (respectively positive) value of Θ' is associated to a high (respectively low) concentration domain and the corresponding "chemical potential" A is given as

$$A = \frac{2\cosh(2\phi)}{[2\cosh(2\phi)+1]^2}\frac{\cosh(4\Theta'-\phi)-\cosh(3\phi)}{\cosh(4\Theta'-\phi)-\cosh(\phi)} \tag{47}$$

A simple physical meaning can be also given to the angle Θ'. One can define the value of the half-width L of the domain as the distance from the center of the domain at which the concentration equals the half sum of the two extreme values (in the center of the domain and at infinity). A simple calculation yields the value of L as

$$L = \frac{1}{2\phi} \operatorname{Arccos}[\cosh(2\Theta' - \phi) + 2] \tag{48}$$

For large domain sizes ($\Theta' \to \pm\infty$), the above equation can be approximated and the half-width L is simply given as the ratio of the two angles:

$$L \cong \frac{|\Theta'|}{\phi} \tag{49}$$

In the limit of infinite domain size, a single kink solution (with two possible orientations) is obtained which connects the two previously found coexistence phases [Eq. (20)]. As in the case of the CH equation, it can be parametrized using a hyperbolic tangent as

$$\rho_k^{\pm} = \frac{-1}{2K} [1 \pm \tanh(\phi) \tanh(k\phi + \Psi)] \tag{50}$$

where $\tanh(\phi) = (-4K - 3)^{1/2}$ and the symbol "+" refers to the two orientations. In this case, A takes the previously found critical value A_c for which the two hyperbolic points of the phase portrait (Fig. 4) are exceptionally connected by the above solution.

5. DYNAMICS

In this section, some results are described concerning the dynamics of this model and which are intended to be an illustrative example of its interest. This is, however, far from being an exhaustive review of what can be made and some interesting points have still to be worked out. The present study concerns the spinodal region and shows some new results about the nonlinear regime.

They are based partly on numerical simulations and for that purpose the evolution equation (7) has been replaced by a numerical scheme in which the time variable is discretized. The time step τ is chosen constant and of a sufficiently small value that no strong departure from the original

Eq. (7) could appear during the time of simulation. Time evolution was then computed using the following algorithm:

$$\rho_k(t+\tau) = \rho_k(t) + \tau[A_{k+1}(t) + A_{k-1}(t) - 2A_k(t)] \tag{51}$$

where $A_k(t)$ is the "chemical potential" at site k and time t:

$$A_k(t) = \rho_k(t)[1 + K\rho_{k+1}(t) + K\rho_{k-1}(t) - K\rho_{k+1}(t)\,\rho_{k-1}(t)] \tag{52}$$

The right-hand side of Eq. (51) has the form of a discrete Laplacian. This, together with the fact that the time step τ can be given rather large values, contributes to make Eq. (51) a fast algorithm for the simulation of phase separation dynamics.

In the spinodal regime, numerical simulations have been performed for different values of mean concentration and temperature, all showing that also the dynamics is very close to a Cahn–Hilliard-type behavior. Although no mathematical proof of the equivalence between both dynamics can be given, this seems to be a reasonable hypothesis. For that reason, the present model could be considered as a discrete version of the CH equation on which both precise numerical and analytical results are available. A typical evolution of the model in the spinodal regime as computed from Eq. (51) is shown in Fig. 7. Starting from an unstable homogeneous profile, a perturbation grows out of an initially small random noise (Fig. 7a) and imposes a well-defined wavelength throughout the system compatible with the linear stability analysis, as can be checked in Fig. 2. At a later time (Fig. 7b), the perturbation saturates within the equilibrium values of the concentration and a further evolution of the profile occurs only through coalescence of neighboring domains (Fig. 7c). In this late stage, the typical growth law of the domain size was found to be compatible with a logarithmic time dependence, reflecting the one-dimensional character of the model.

Beside these standard results, some other information can be gained due to the numerical precision of these simulations: the spatial variations of the "chemical potential" $A_k(t)$ can be studied and in the late stages show the same kind of behavior as in Fig. 8 over orders of magnitude. From this observation, which was verified in all the simulations, qualitative statements can be made about the behavior of time-dependent profiles in this regime: (a) for such values of mean concentration and a sufficient coarsening, the high-concentration domains can be given independently a well-defined value of the "chemical potential" which depends only on their size. This is valid at any time except perhaps when the domain is about to disappear. A similar statement can be made at high concentrations by exchanging the roles of the two phases. (b) The current between neigh-

boring domains can be considered as constant across the dominant low-concentration phase; it depends on the difference between the "chemical potentials" and on the distance between domains. (c) In spite of the relative stability of the profile and the small dispersion in the distribution of domain sizes, the system cannot be generally considered as globally near a single periodic stationary solution, as the correlation length of the "chemical potential" is hardly larger than the mean domain size.

In view of these observations, it seems more appropriate to describe such a system as a collection of domains of high concentration with an exchange of matter between nearest neighbors depending on a size-depend-

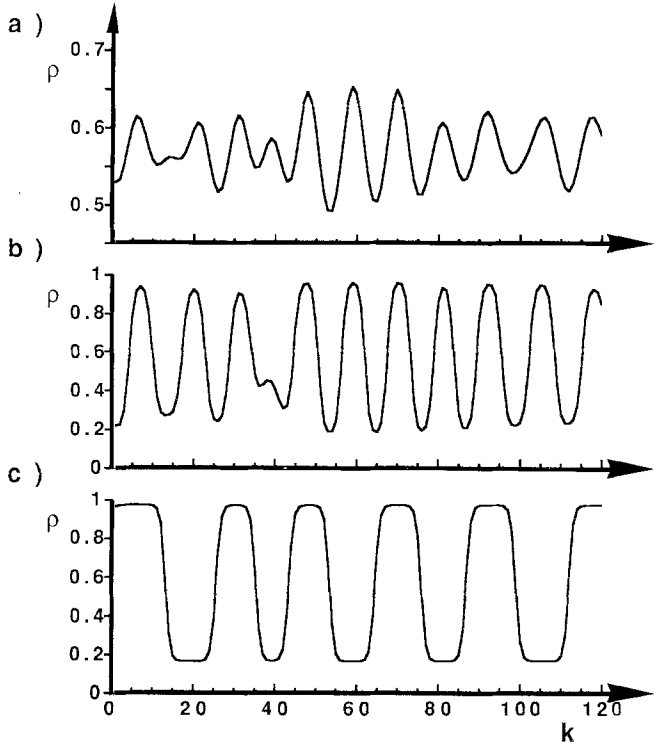

Fig. 7. Snapshots of a typical time evolution of the model in the spinodal region obtained by numerical simulations ($K = -0.875$). The initial configuration consists of homogeneous profile at concentration $\rho = 0.5714$ plus a random noise of small amplitude (10^{-4}). The computation was performed on a box with 252 sites and periodic boundary conditions. The three pictures correspond to the same window of 120 sites for three different times: (a) $t = 125$; the system is still in the initial linear regime, but the most unstable mode is already dominant (see Fig. 2). (b) $t = 1250$; most of the initial domains still survive and saturate around the equilibrium values of the density. (c) $t = 1.25 \times 10^6$; the system now evolves by coalescence of neighboring domains. The mean size of domains follows a logarithmic growth law.

ent "chemical potential." In this interpretation, the approximate periodicity of the profile is explained by the homogeneity of the initial profile and the periodicity of the dominant fluctuation which is established in the linear stage. The small observed dispersion in the distribution of domain sizes then should be a consequence of the strong size dependence of the lifetime and of a finite time of computation. Finally, this is also consistent with the absence of diffusion in the system, which should prevent a new long-distance ordering in the late stages.

This interpretation is used in the following as a working approximation scheme and leads to an expression for the exponents characterizing the instability of stationary solutions. Quantitative support then will be given to this interpretation by a direct comparison to numerical values which can be precisely computed for periodic solutions. For this reason, only the simplest unstable modes will be considered, which correspond to a doubling of the spatial wavelength of the stationary profile under consideration. The method could nevertheless apply to other unstable modes, giving exponents of the same order.

One considers a periodic or quasiperiodic bounded stationary solution as the initial profile of an infinite system. In order to keep with the simplest approximation, the interface thickness will be neglected and the concentrations in both phases taken as the coexistence values [Eq. (20)]. In this approximation, a profile will be described as a succession of domains of

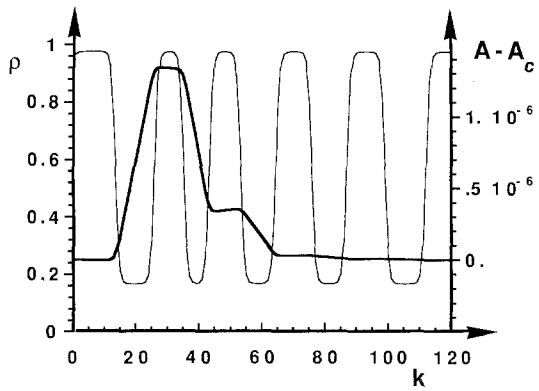

Fig. 8. Spatial variation of the "chemical potential" A in the late stage of spinodal decomposition. The value of $A - A_c$ (A_c is the equilibrium value) has been superimposed on the concentration profile of Fig. 6c. For these values of concentration and coarsening, the system is well approximated by considering it as a collection of high-concentration domains in a low-concentration phase. Each domain can be given a well-defined value of "chemical potential" which depends only on its size. The exchange of matter between neighboring domains is due to a constant current in the low-concentration phase proportional to the difference between "chemical potentials."

high concentration ρ_+ and half-width L_+ alternating with domains of low concentration ρ_- and half-width L_-. The wavelength $\mathscr{L}$ and mean concentration ρ of the stationary solution will be here approximated as

$$\mathscr{L} = 2(L_+ + L_-) \tag{53}$$

$$\rho = \frac{\rho_+ L_+ + \rho_- L_-}{L_+ + L_-} \tag{54}$$

At time $t = 0$, a small perturbation is added with zero concentration and a wavelength exactly twice that of the initial stationary solution. Then the system starts to evolve, keeping this new wavelength at all times. Now, if the above considerations are correct, the only noticeable effect of the perturbation in the linear regime is to modify the sizes of high-concentration domains. When applied to the case of a doubling of the wavelength, this fully specifies the nature of the perturbation; mean concentration and wavelength being fixed, growing domains of high concentration must alternate with shrinking ones, and their half-widths evolve in time according to, respectively,

$$L_+^{(1)}(t) = L_+ + \delta L_+(t) \tag{55a}$$

$$L_+^{(2)}(t) = L_+ - \delta L_+(t) \tag{55b}$$

where $\delta L_+(t)$ is a small time-dependent variation whose initial value depends on the amplitude of the perturbation. Within the present approximations, a well-defined value of "chemical potential" A can be given to each domain using the expression for isolated domain solutions [Eq. (47)]. In the linear regime when the size variations remain small, its time evolution is related to that of the half-widths as

$$\delta A_+(t) = \left.\frac{\partial A}{\partial L}\right|_{L_+} \delta L_+(t) \tag{56}$$

where the derivative has to be calculated from Eq. (47) and evaluated at $L = L_+$. The difference in the chemical potentials of neighboring domains induces a flow of matter between them, and the current, considered as constant throughout the low-concentration phase, then reads

$$J_{(1\to 2)}(t) = -\frac{1}{L_-}\delta A_+(t) \tag{57}$$

Now integrating the evolution equation (7) over one interface leads to the equation for the time evolution for the half-widths as

$$(\rho_+ - \rho_-)\frac{\partial}{\partial t}[\delta L_+(t)] = -\frac{1}{L_-}\left.\frac{\partial A}{\partial L}\right|_{L_+} \delta L_+(t) \tag{58}$$

This equation can be readily solved, showing that the perturbation grows exponentially in the linear regime with a characteristic exponent λ_+ which reads

$$\lambda_+ = -\frac{1}{(\rho_+ - \rho_-)\, L_-} \left.\frac{\partial A}{\partial L}\right|_{L_+} \tag{59}$$

A similar analysis can be made by exchanging the role of high- and low-concentration phases so that finally two different unstable modes are found for each stationary solution, associated to a doubling of the wavelength. In the limit of large domain size, Eq. (47) can be approximated and the two exponents expressed as

$$\lambda_+ = 32\phi \frac{\mathrm{th}(\phi)^2}{3 - \mathrm{th}(\phi)^2} \frac{\exp\{-2\phi(L_+ - 2)\}}{L_-} \tag{60}$$

$$\lambda_- = 32\phi \frac{\mathrm{th}(\phi)^2}{3 - \mathrm{th}(\phi)^2} \frac{\exp\{-2\phi(L_- + 2)\}}{L_+} \tag{61}$$

where $\phi = \mathrm{Arctanh}[(-4K-3)^{1/2}]$ is the value obtained in the limit of infinite domain sizes. Now using Eqs. (60) and (61) together with Eqs. (53) and (54) gives the dependence of the relative stability of stationary solutions on their wavelength and mean concentration. In particular, it must be noted that the exponents have a wavelength dependence in $e^{-\alpha \mathscr{L}}/\mathscr{L}$, $\alpha > 0$, hence the same as what was already estimated for a symmetric solution of the CH equation, using a tight-binding method.[12] This is perhaps an indication that both models are equivalent also from a dynamical point of view. It also proves that stable stationary solutions must have an infinite wavelength, thus eliciting the hyperbolic tangent profile [Eq. (50)] as the unique stable equilibrium solution in the spinodal domain.

The explicit dependence on the concentration is also found, and can be considered as exponential over a wide range of values. It has been plotted in Fig. 9 for two different wavelengths and the same value of temperature. This indicates that the two different modes are alternatively dominant as the concentration is varied, the description in terms of interacting domains of the minority phase appearing to be always the most appropriate. The exponents for the same periodic solutions have also been obtained numerically, by computing directly the eigenvalues of the linearized evolution operator of Eq. (7). In the case of periodic stationary solutions and wavelength-doubling modes, the problem reduces to the finding of the positive eigenvalues of a finite matrix which has been diagonalized numerically. The phase Ψ with the lattice was tested on a smaller system to be of very weak influence and the eigenvalues were computed only for particular

values when the two modes can be separated by an additional requirement of symmetry in the perturbation. Results are plotted in Fig. 9 and show an almost perfect agreement with the values obtained from Eqs. (60) and (61) in a large range of concentration. The computed exponents are also found to be drastically enhanced for the largest and smallest values of concentration. These values correspond to the limit of existence of stationary solutions for a fixed wavelength and the enhancement is due to the disappearance of domains in the minority phase. Such an effect was discarded in the derivation of Eqs. (60), (61) and a more careful calculation should be made along the same lines which takes into account both the finite width of the interface and the size dependence of concentration inside domains.

However, the very good accuracy of Eqs. (60), (61) in their domain of validity, even for rather small values of wavelength and within drastic approximations, gives strong support to the idea that the description in terms of interacting domains is the correct one already for stationary solutions and *a fortiori* for time-dependent profiles in the late stages of spinodal

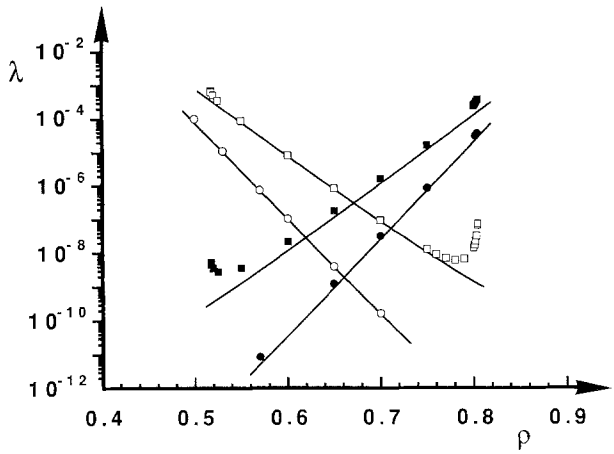

Fig. 9. Exponent λ of the unstable modes around stationary solutions, represented as a function of concentration, for two values of the wavelength $\mathscr{L}$: upper curves and square points: $\mathscr{L}=30$; lower curves and circles: $\mathscr{L}=42$. Here $K=-0.785$. Two modes are considered, associated to a doubling of the wavelength; white dors and associated curves: the system is considered as interacting high-concentration domains; black dots and associated curves: the same system is considered as interacting low-concentration domains. The dots show the numerical values obtained by linearization of the evolution operator around a given stationary solution. Solid lines are the analytical results from Eqs. (60) and (61), showing a very good agreement in the central domain of concentration. The strong enhancement of the numerical values on both sides is due to the vanishing in size and amplitude of domains of the minor phase.

decomposition. This was checked, for numerical reasons, only for a particular set of perturbations and a further study of unstable modes with larger wavelength could be of interest. It can be also added that the above description also holds beyond the linear regime when the difference in size between domains is not small. It was also verified on a few examples that this gives also correct predictions for the exponents which can be defined on time-dependent profiles such as in Fig. 8.

6. CONCLUSION

A one-dimensional spatially discrete model has been proposed which describes a dynamical process of phase separation with conserved order parameter. Although related from the beginning to an anisotropic lattice gas and in spite of the absence of a well-defined free energy functional, strong analogies with the Cahn–Hilliard equation have been found. In particular, both the structure of stationary solutions and their dynamic stability were found to be comparable, giving support to the idea that the present model is a correct discrete version of the Cahn–Hilliard equation. Furthermore, new results were presented on both static and dynamical aspects of phase separation, showing the large potential interest of such a model: First, a full parametrization in terms of elliptic variables provided a clear picture of the stationary solutions, showing the particular position of spinodal and coexistence curves among bounded solutions. Then, the dynamics of spinodal decomposition was investigated in the strongly nonlinear regime; using previously found stationary solutions as an input for characterizing single domains, this study has shown that a system undergoing spinodal decomposition is better described as a rescaled system of domains with nearest-neighbor interactions, rather than by an approximate periodic stationary solution. At the same time, this provided an example of the interest of such a model in which new results can be found using the interplay between accurate numerical simulations and analytical results.

A number of further developments can be thought of, roughly classified along two directions:

On a fundamental level, the relation to both the underlying lattice gas model and the Cahn–Hilliard equation should be investigated in more detail. This model could provide new insights on the nature of the approximations which lead to a factorization of correlation functions [Eq. (5)]; the relation to continuous models could be also considered from a more mathematical point of view. In that way, a better understanding of the nature of the multiplicity of factorization of the current operator could be a key point.

More physically oriented developments of the model can be also

proposed which could make use of the possibility of playing on both analytical and numerical levels to test some new ideas, as in the case of spinodal decomposition, but for different regimes of the dynamics (metastability, critical dynamics, etc.) or different initial conditions (macroscopic fluctuations of concentration).[19] Other, more finely tuned phenomena could be also derived from the precise knowledge of the set of stationary solutions: for instance, the jump from the linear to the nonlinear regime in intermediate stages of phase separation may be found to depend strongly on the equilibrium solutions which can be approached by the system and influence the structure of the residual noise in the late stages.

Finally, extensions of that kind of model to higher dimension also have to be considered. In view of the present numerical and analytical state of the art, a two- or three-dimensional equivalent of that model certainly would be of great interest. Preliminary numerical results on simple generalizations were already obtained, but an equivalent of Eqs. (17) and (18) has still to be found to allow for the construction of a model of phase separation solvable in higher dimensions.

REFERENCES

1. J. W. Cahn and J. E. Hilliard, Free energy of a nonuniform system. I. Interfacial free energy, *J. Chem. Phys.* **28**:258 (1958).
2. J. W. Cahn, Phase separation by spinodal decomposition in isotropic systems, *J. Chem. Phys.* **42**:93 (1965).
3. J. S. Langer, M. Bar-on, and H. D. Miller, New Computational method in the theory of spinodal decomposition, *Phys. Rev. A* **11**:1417 (1975).
4. I. M. Lifshitz and V. V. Slyosov, The kinetics of precipitation from supersaturated solid solutions, *J. Phys. Chem. Solids* **19**:35 (1961).
5. D. A. Huse, Corrections to late-stage behavior in spinodal decomposition: Lifshitz Slyosov scaling and Monte Carlo simulations, *Phys. Rev. B* **34**:7845 (1986).
6. H. Furukawa, A dynamical scaling assumption for phase separation, *Adv. Phys.* **34**:703 (1985).
7. J. D. Gunton, M. San Miguel, and P. S. Sahni, in *Phase Transitions and Critical Phenomena*, Vol. 8, C. Domb and J. L. Lebowitz, eds. (Academic Press, New York, 1983).
8. J. L. Lebowitz, E. Orlandi, and E. Presutti, A particle model for spinodal decomposition, *J. Stat. Phys.* **63**:933 (1991).
9. H. van Beijeren and L. S. Schulman, Phase transitions in lattice-gas model far from equilibrium, *Phys. Rev. Lett.* **53**:806 (1984).
10. J. Krug, J. L. Lebowitz, H. Spohn, and M. Q. Zhang, The fast rate limit of driven diffusive systems, *J. Stat. Phys.* **44**:535 (1986).
11. O. Penrose, A mean-field equation of motion for the dynamic Ising model, *J. Stat. Phys.* **63**:975 (1991).
12. J. S. Langer, Theory of spinodal decomposition in alloys, *Ann. Phys.* (N.Y.) **65**:53 (1971).
13. S. Puri and Y. Oono, Effect of noise on spinodal decomposition, . *Phys. A* **21**:L755 (1988).
14. M. Abramowitz and I. A. Stegun, *Handbook of Mathematical Functions* (National Bureau of Standards, Washington, D.C. 1964).

15. P. F. Byrd and M. D. Friedman, *Handbook of Elliptic Functions for Engineers and Scientists*, 2nd ed. (Springer-Verlag, Berlin, 1971).
16. A. Novick-Cohen and L. A. Segel, Nonlinear aspects of the Cahn–Hilliard equation, *Physica D* **10**:277 (1984).
17. A. Novick-Cohen, The nonlinear Cahn–Hilliard equation: Transition from spinodal decomposition to nucleation behavior, *J. Stat. Phys.* **38**:7073 (1985).
18. R. Pandit and M. Wortis, Surfaces and interfaces of lattice models: Mean field theory as an area-preserving map, *Phys. Rev. B* **25**:3226 (1982).
19. M. Kolb, T. Gobron, *J. F.* Gouyet, and B. Sapoval, Spinodal decomposition in a concentration gradient, *Europhys. Lett.* **11**:601 (1990).